ORIGINAL RESEARCH ARTICLE

Electrical and Structural Characterization of Poly(3-hexylthiophene)–Polydiphenylamine Blends Synthesized on Various Conductive Substrates

MAYARA MASAE KUBOTA[1] and HENRIQUE DE SANTANA [1,2]

1.—Departamento de Química, CCE, Universidade Estadual de Londrina, Londrina, PR 86051-990, Brazil. 2.—e-mail: hensan@uel.br

With the aim of assessing whether polydiphenylamine (PDPA) can be used as an inductor layer for stabilizing the radical cation in the polymer matrix of poly(3-hexylthiophene) (P3HT), as used in photovoltaic devices, interphases between P3HT and PDPA films were prepared electrochemically on platinum (Pt), tin-doped indium oxide (ITO), and gold (Au) electrodes in lithium perchlorate-acetonitrile (LiClO$_4$-ACN) solution, being denoted as Pt/PDPA:P3HT, ITO/PDPA:P3HT, and Au/PDPA:P3HT, respectively. To characterize the interphases deposited on the different electrodes, Raman spectroscopy was used to monitor the behavior of the segments in the blend matrix compared with homopolymer films deposited on the different conducting electrodes, to study the stability of the quinone and semiquinone segments of PDPA and P3HT. Bode phase diagrams obtained by electrochemical impedance spectroscopy (EIS) were used to verify the prepared systems as a function of time since preparation. It was found that the polaron structure (oxidized thiophene ring radical cation segments) was stable for 97 h when the blend was synthesized under controlled temperature (22°C) conditions at constant potential of 1.70 V applied for 60 s to the surface of the Pt electrode. For the blends synthesized on ITO and Au, these conditions resulted in greater stabilization of the bipolaron structure (dication segments). These findings reveal the effect of PDPA induction over the P3HT layer in stabilizing the semiquinone and quinone forms, compared with interfaces formed solely by homopolymers in contact with the different electrodes.

Key words: Poly(3-alkylthiophenes), PDPA, electrochemical impedance spectroscopy, organic photovoltaic cells

INTRODUCTION

Semiconductor polymers can be switched from insulating to conducting nature by adding charge-transfer agents (dopants) that, by oxidizing or reducing the conjugated system, change the final properties of the polymer.[1] This kind of process induces a transition from an aromatic to quinone form, thereby allowing the formation of radical cation and dication in the polymer chain.[2] In this class of polymers, redox reactions are responsible for the electrical conductivity and electrochemical and electrochromic properties.[3–8]

Poly(3-alkylthiophenes) (P3ATs) are used in advanced organic devices due to their advantages of good thermal and chemical stability, thermochromism, luminescence, solubility, and production of stable interfaces with the metal electrodes used in electronics. Furthermore, these materials can be easily deposited as polymer films over different conductive substrates and can undergo

reversible changes between electrically insulating and semiconducting states.[9–12]

In addition, P3ATs are acknowledged to be highly photosensitive, making them an excellent choice for use in photovoltaic cell devices, since they readily absorb visible light. When the semiconductor is modified by chemical treatment (for example, chemical or electrochemical doping), it can acquire singular properties at the substrate–polymer interface, which in turn affect the behavior of the organic optoelectronic device. Thus, characterization of the structure of these materials is necessary to understand what happens during the electrochemical process, and in particular the conditions under which electrochemical synthesis is carried out.[13,14]

In a study by Batista et al.,[15] the authors used poly(3,4-ethylenedioxythiophene) polystyrene sulfonate (PEDOT:PSS) to form the active layer at the interface for application in organic photovoltaic (OPV) cells. They demonstrated the stability of the radical cation over time in the ITO/PEDOT:PSS/P3MT system, which is important for improving the electrical and optical properties of OPV cells.

To study an efficient alternative for the active layer in OPV cells that would provide enhanced stability of the radical cation segment compared with PEDOT:PSS, we chose PDPA for insertion into the interface with P3AT. This choice was based on the fact that PDPA has good redox and ambient stability properties, since the semiquinone-based stabilization of PDPA could provide an inductor layer for P3AT segments, thereby helping to improve the electrical and optical properties of OPV cells.[16]

The use of P3ATs together with PDPA has resulted in improved properties for these materials. Bento et al.,[17] studied electrochemical synthesis of blends of PDPA and poly(3-octylthiophene) and poly(3-methylthiophene) on a platinum electrode, reporting variations in the optical and electrical properties compared with the respective homopolymers. Using Raman spectroscopy, these variations were found to result from stabilization of radical cation and dication species in the polymer chain. Other researchers have reported optical and electrical modifications due to copolymerization between P3ATs [poly(3-methylthiophene) (P3MT), poly(3-hexylthiophene) (P3HT), and poly(3-octylthiophene) (P3OT)] after modifying the electrochemical synthesis parameters, such as the support electrolyte, substrate, and temperature. In these studies, *in situ* and *ex situ* Raman spectroscopy and electrochemical impedance spectroscopy (EIS) provided valuable tools for characterizing the material formed.[13,17,18]

To better understand whether the interface between PDPA and P3HT deposited on different conductive substrates stabilizes the radical cation segments in the P3HT polymer matrix, and whether the structure of the PDPA could favor this stabilization, PDPA film was electrochemically synthesized between P3HT and platinum, ITO, and Au electrodes in $LiClO_4$ solution in acetonitrile. In terms of the experimental variables, the results showed that the stability of the radical cation segments is higher if, during synthesis, the temperature is kept at 22°C, since at ambient temperature the semiquinone segments undergo spontaneous conversion to quinone segments,[19] revealing the structural instability inside the polymer matrix.

Thus, Pt/PDPA:P3HT, ITO/PDPA:,P3HT and Au/PDPA:P3HT interphases were obtained electrochemically and their performance compared with the systems consisting only of homopolymers deposited on the conductive electrodes. Bode phase diagrams produced by EIS were studied as a function of time since synthesis to determine the phases present at different times. This was complemented by *ex situ* Raman spectroscopy to characterize the aromatic, radical cation, and dication segments in the as-prepared interphases.

EXPERIMENTAL PROCEDURES

Reagents

3-Hexylthiophene monomer $(C_{10}H_{16}S)$ and diphenylamine $[(C_6H_5)_2NH]$ were supplied by Sigma-Aldrich and used as received. The support electrolyte was lithium perchlorate ($LiClO_4$, 99% pure; AcrosOrganics), and the solvent was acetonitrile [ACN, high-performance liquid chromatography (HPLC) grade, 99.5% pure; JT Baker].

Electrochemical Synthesis and Cyclic Voltammetry

PDPA was synthesized by cyclic voltammetry, varying the potential between 0.60 V and 1.20 V in steps of 100 mV s^{-1}, in solution of 0.10 mol L^{-1} DPA in $LiClO_4$-ACN onto Pt, Au, and ITO electrodes for 60 cycles at 22°C. The electrode with PDPA film was removed at a potential of 1.2 V and kept at ambient temperature.

P3HT films were synthesized electrochemically by chronoamperometry, applying a potential of 1.70 V and 1.80 V to the platinum, gold, and ITO for 65 s in solution of 3-hexylthiophene monomer at concentration of 0.04 mol L^{-1} in $LiClO_4$-ACN. The temperature was kept constant at 22°C during synthesis. The electrodes with P3HT films were removed from the solution at a potential of 1.70 V or 1.80 V and kept at ambient temperature.

To prepare a layer of P3HT on the substrate/PDPA interphase, PDPA was initially synthesized on the substrate and the P3HT film was subsequently synthesized on this material under the aforementioned synthesis conditions. After deposition on the electrodes, the films were kept at ambient temperature pending characterization after the times stated in this study had elapsed.

Both chronoamperometry and cyclic voltammetry were performed using a potentiostat/galvanostat

Electrical and Structural Characterization of Poly(3-hexylthiophene)–Polydiphenylamine
Blends Synthesized on Various Conductive Substrates

(Autolab PGSTAT 302 N) coupled to a microcomputer running NOVA 1.8 software. The auxiliary electrode was a platinum plate with area of 0.50 cm^2. The potentials were determined with reference to Ag/AgCl in a Luggin capillary in 0.10 mol L^{-1} solution of lithium perchlorate in acetonitrile (LiClO$_4$-ACN).

Raman Spectroscopy

Ex situ Raman spectra were obtained using a portable Raman spectrometer (Advantage532, DeltaNu) with excitation at 532 nm and resolution of 8 cm^{-1}. DeltaNu NuSpec software and baseline resources were used to remove background fluorescence.

Electrochemical Impedance Spectroscopy (EIS)

Impedance diagrams were obtained using a potentiostat (Autolab PGSTAT 302 N) with the FRAM32 impedance module, varying the frequency from 100 kHz to 0.01 Hz. Open-circuit stabilization potentials (E_{OC}) were reached when the E_{OC} remained constant (± 5 mV) for 30 min, the time necessary to reach the stationary state in which the current remained constant.

RESULTS AND DISCUSSION

Preliminary experimental results revealed that the temperature at which the homopolymers and blends were synthesized electrochemically on the conductive substrates would first have to be defined. Indeed, in terms of the experimental variables, the results showed that the stability of the radical cation segments of poly(3-hexylthiophene) was initially greater if, during synthesis, the temperature was maintained at 22°C, because at room temperature the radical cation segments suffered spontaneous conversion into dication segments, revealing the structural instability of the polymer matrix. In experiments in which the synthesis temperature was not controlled, greater presence of dication segments was observed in the various systems studied shortly after synthesis. Considering this fixed experimental condition, the main objective of this work is to evaluate the capacity of polydiphenylamine as an inducing layer to stabilize the radical cation in the polymeric matrix of poly(3-hexylthiophene), and on which conductive substrate this effect would be more effective. Thus, studies on the characterization of systems with the homopolymers on different substrates are presented first, followed by the blend systems.

Raman spectra were obtained at different times after preparation with the aim of characterizing the stability of the PDPA quinone structures, i.e., the radical cation and dication segments at the interfaces formed in the Pt/PDPA, ITO/PDPA, and Au/PDPA systems.

Figure 1a shows the Raman spectra for the Pt/PDPA system, obtained at different times. After synthesis, predominant bands characteristic of the PDPA radical cation were observed at 1203 cm^{-1}, 1322 cm^{-1}, and 1530 cm^{-1}, being assigned to C–H angular deformation, C–C interring stretching, and C–N stretching. These segments exhibited a widened absorption band between 450 nm and 490 nm in the ultraviolet–visible (UV–Vis) spectrum of the composite, allowing the sample under excitation at 532 nm to undergo resonance Raman intensification.[2]

However, irrespective of the predominance of intense bands related to radical cation segments in the resonance Raman spectrum, the deconvolution technique can be used to verify other segments in the polymer matrix. Based on the components in the widened band centered at 1608 cm^{-1} and related to C–C stretching of the PDPA aromatic ring,[20] as shown inset in Fig. 1a, b, it is possible to see this stretching mode related to the dication, aromatic, and radical cation segments at wavenumbers of 1566 cm^{-1} to 1589 cm^{-1}/1572 cm^{-1}, 1611 cm^{-1}/1607 cm^{-1}, and 1627 cm^{-1}/1619 cm^{-1}.[21]

In general, at other times after synthesis, the Raman spectra for the Pt/PDPA system showed a loss of intensity in the 1322 cm^{-1} band related to radical cation segments. Furthermore, in the spectrum obtained 97 h after synthesis, there is an intense band at 1369 cm^{-1}, which can be attributed to C–C interring stretching, and a band at 1180 cm^{-1}, related to C–H angular deformation, both characteristic of the dication segment.[2]

Along with the reduction observed in the radical cation segments in the polymer matrix as time progressed, the bands related to dication segments also appeared with good spectral intensity. This can be explained by the fact that the dication segments exhibited a widened absorption band centered at 588 nm, causing the preresonance Raman effect in the spectrum with excitation at 532 nm. This result may indicate that, at the interface with platinum, a disproportionation reaction occurs spontaneously in the radical cation segments to form dication and aromatic segments in PDPA.[2]

Figure 1b and c show the Raman spectra of the ITO/PDPA and Au/PDPA systems obtained at different time intervals. After synthesis, predominant bands corresponding to the radical cation segments were observed, whereas subsequently there were no significant variations in the spectra up to 97 h after synthesis. This was considered to show the high stability of the radical cation segments at the interfaces with these ITO and Au electrodes.

Figure 2 shows Bode phase diagrams constructed using data obtained by EIS for the Pt/PDPA, ITO/PDPA, and Au/PDPA systems in 0.100 mol L^{-1} LiClO$_4$-ACN solution. The EIS measurements were taken at open-circuit potential (OCP) and constant temperature of 22°C at different times (0 h, 1 h, 5 h,
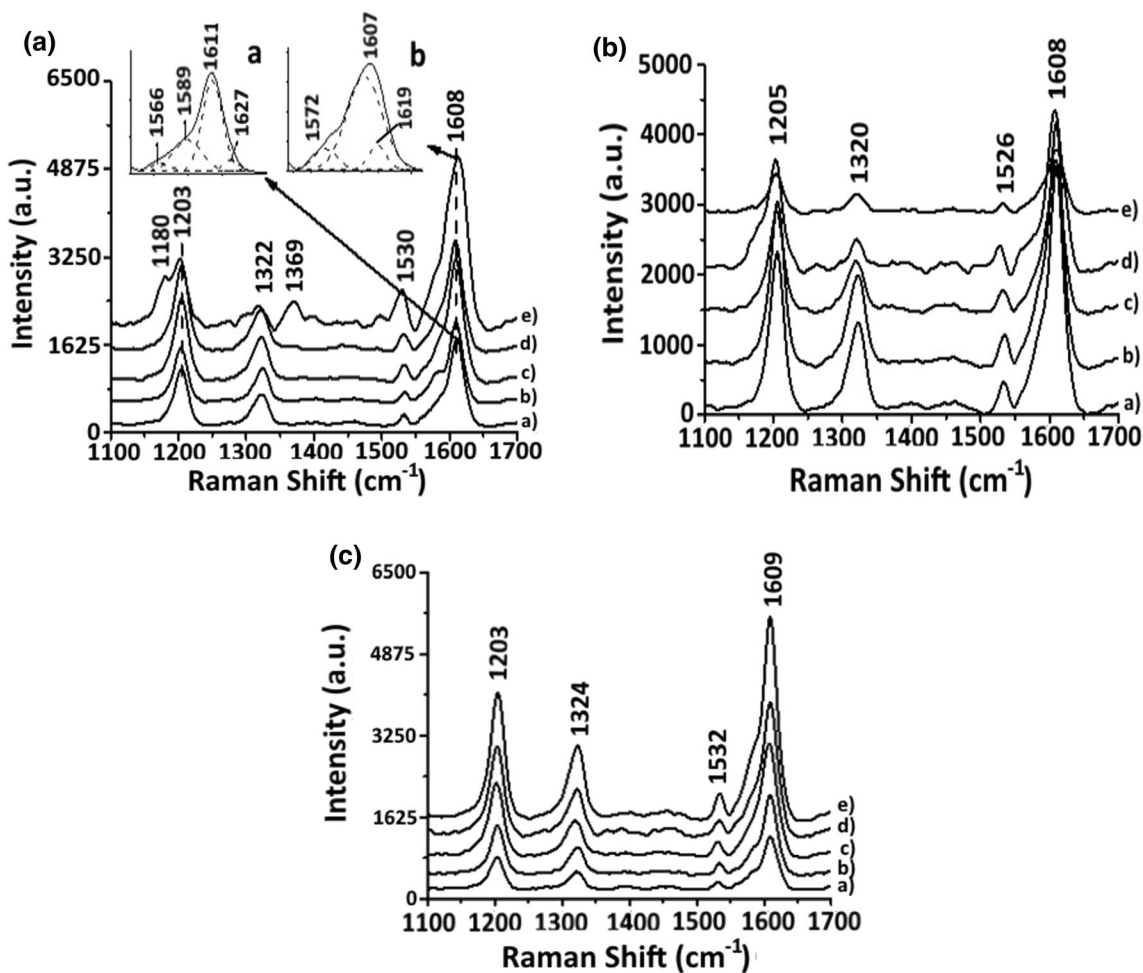
Fig. 1. Raman spectra with excitation at 532 nm of (a) Pt/PDPA, (b) ITO/PDPA, and (c) Au/PDPA systems at (a) 0 h, (b) 1 h, (c) 5 h, (d) 48 h, and (e) 97 h after synthesis. Inset: deconvoluted Raman spectra of Pt/PDPA system after (a) 0 h and (b) 97 h.

48 h, and 97 h) after preparation of the films on Pt, ITO and Au electrodes.

The diagrams for the Pt/PDPA system (Fig. 2a) show a single widened phase at ~ 2.31 Hz at time 0 h, which is displaced to ~ 1.18 Hz after 48 h. This phase relates to the bipolaron conduction charge-transfer process,[22] indicating that the dication segments in the PDPA at the interface with platinum remained stable over the assessment time, due to the large amount of such segments in the polymer matrix. On the other hand, this result could confirm that, in the polymer matrix, radical cation segments in the PDPA must be present at a much lower quantity, since the EIS diagram does not show any indications of the phase characteristic of these segments, despite the fact that the resonance Raman spectrum confirms their presence in the polymer matrix.

It was not possible to obtain EIS measurements for the Pt/PDPA system after 97 h, since the polymer film was completely soluble in 0.100 mol L^{-1} LiClO$_4$-ACN, perhaps because of the increased hydration of the film due to an increase in the quantity of dication segments in the PDPA film

matrix, as shown by the Raman spectroscopy results.

Figure 2b and c show Bode phase diagrams for the ITO/PDPA and Au/PDPA systems. At all assessment times, a single phase was observed at ~ 0.014 Hz, being related to polaron conduction charge-transfer processes,[13] indicating that the radical cation segment was stable throughout the assessment time, in contrast to the platinum system.

Raman spectra were obtained at different times after electrochemical synthesis with the aim of characterizing the quinone structures in P3HT, i.e., the radical cation and dication segments at the interfaces formed by the Pt/P3HT, ITO/P3HT, and Au/P3HT systems.

Figure 3a shows the Raman spectra for the Pt/P3HT system, obtained at different time intervals. After synthesis, bands were observed at 1376 cm^{-1}, characteristic of C–C stretching of the ring, and at 1453 cm^{-1}, characteristic of C=C symmetric stretching of the thiophene ring. The latter band shifted to 1457 cm^{-1} as time progressed, revealing an alteration in the stability of the quinone segments.[23]

Electrical and Structural Characterization of Poly(3-hexylthiophene)–Polydiphenylamine
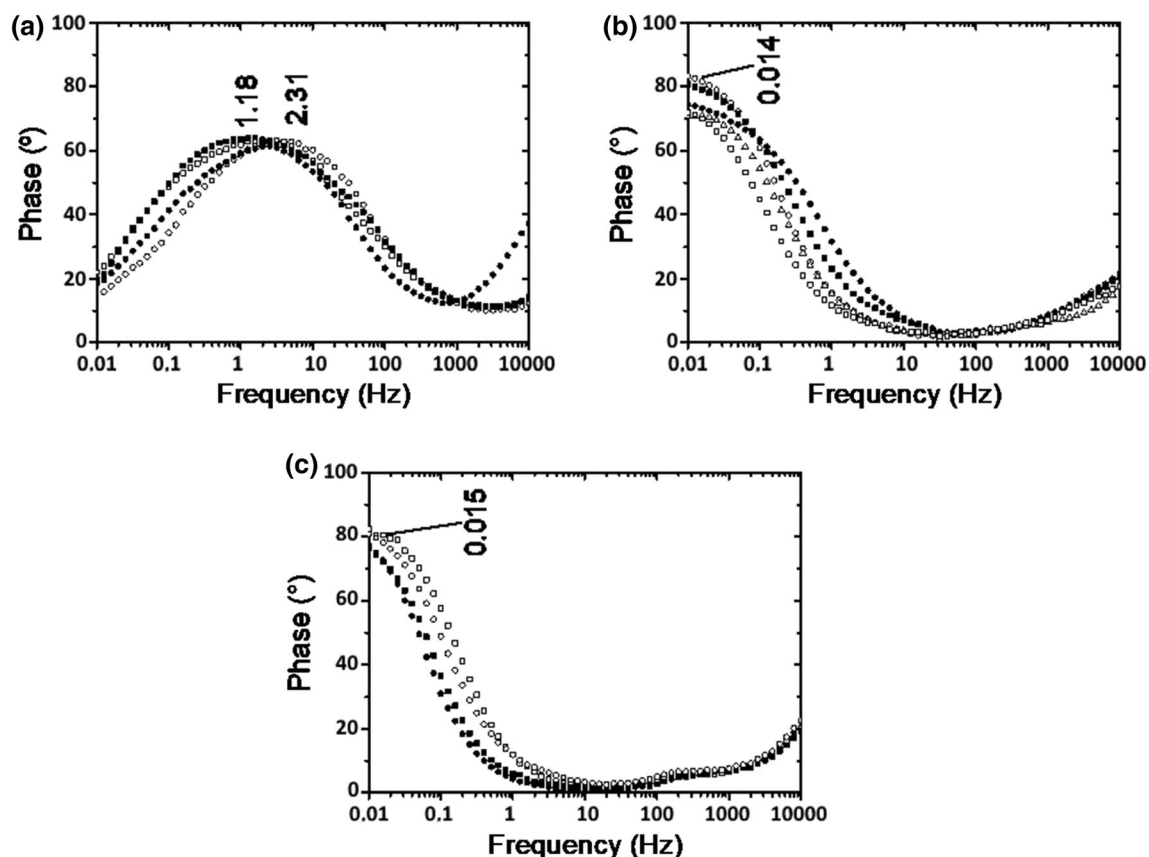Blends Synthesized on Various Conductive Substrates

Fig. 2. Bode phase diagrams at open-circuit potential for (a) Pt/PDPA, (b) ITO/PDPA and (c) Au/PDPA systems at 0 h (empty circle), 1 h (filled circle), 5 h (empty square), 48 h (filled square), and 97 h (empty triangle) after electrochemical synthesis.

The band at 1457 cm^{-1} is associated with the parts played by the radical cation, dication, and aromatic thiophene ring segments, which coexist in the P3HT polymer matrix. Therefore, this band was deconvoluted to observe the behavior of these segments. As shown in the insets to Fig. 3a, b, after deconvolution, this band shows dication and radical cation thiophene ring segments represented by signals at wavenumbers of 1424 cm^{-1}, 1454 cm^{-1}, and 1473 cm^{-1}, and 1427 cm^{-1}, 1452 cm^{-1}, 1469 cm^{-1}, respectively.[23, 24]

Despite the displacements in frequency observed as a function of time due to constant changes in the segments present in the polymer matrix, an increase in the relative intensity of the band at 1469 cm^{-1} in the deconvoluted spectrum obtained at 97 h, compared with the band at 1473 cm^{-1}, was also observed in the spectrum for the as-prepared film. This could indicate that the radical cation segments reach greater equilibrium with the dication segments in the polymer matrix, increasing the quantity of dication segments as time progresses.

Figure 3b and c show the Raman spectra for the ITO/P3HT and Au/P3HT systems, obtained at different time intervals. In both systems, the same bands already observed also appeared, and the band at 1444 cm^{-1} to 1453 cm^{-1} is displaced to 1455 cm^{-1} to 1457 cm^{-1} as time progresses, leading to a predominance of quinone segments at these interfaces.

As shown in the insets to Fig. 3c–f, the same band, after deconvolution, was slightly displaced compared with the observations at the interface with platinum. Signals were observed at wavenumbers of 1443 cm^{-1} and 1466 cm^{-1}, 1454 cm^{-1} and 1472 cm^{-1}, 1444 cm^{-1} and 1464 cm^{-1}, and 1450 cm^{-1} and 1467 cm^{-1}, related to the dication and radical cation segments of the thiophene ring.[23, 24] This indicates that the radical cation segment reached greater equilibrium with the dication segments in the polymer matrix over a longer time period after synthesis, mainly at the interface with the ITO electrode.

Figure 4 shows the Bode phase diagrams constructed based on the data obtained from EIS for the Pt/P3HT, ITO/P3HT, and Au/P3HT systems.

In Fig. 4a, c, the diagrams obtained at 0 h and 5 h show a phase related to the polaron conduction charge-transfer process at low frequencies (~ 0.035 Hz and ~ 0.021 Hz). However, those obtained during the period from 48 h to 97 h exhibited a widened phase (~ 0.201 Hz and ~ 0.350 Hz) related to polaron and bipolaron conduction charge-transfer processes.[14] These results corroborate the Raman spectrum results, which also showed radical cation
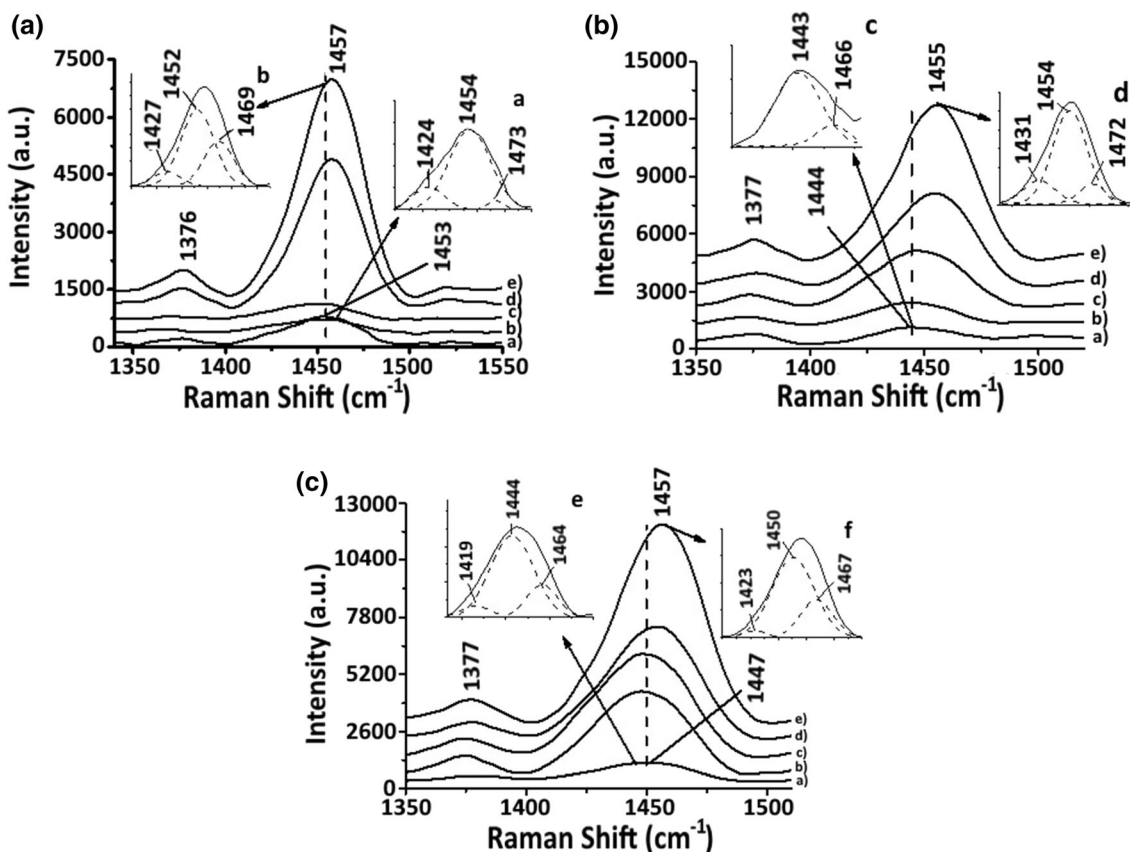
Fig. 3. Raman spectra with excitation at 532 nm of (a) Pt/P3HT, (b) ITO/P3HT, and (c) Au/P3HT systems at (a) 0 h, (b) 1 h, (c) 5 h, (d) 48 h, and (e) 97 h after electrochemical synthesis. Inset: deconvoluted Raman spectra for Pt/P3HT system after (a) 0 h and (b) 97 h, ITO/P3HT system after (c) 0 h and (d) 97 h, and Au/P3HT system after (e) 0 h and (f) 97 h.

and dication bands after deconvolution of the band at 1457 cm^{-1}.

Figure 4b shows two phases from 0 h to 5 h at approximately 0.016 Hz, related to the polaron conduction charge-transfer process, and at high frequencies, related to the bipolaron conduction charge-transfer process. After an interval of 5 h, the system exhibited instability, with a predominance of the widened phase at high frequencies, indicating the predominance of the dication segment as from 48 h after synthesis.[25]

Experiments were conducted on the systems to determine whether the presence of PDPA at the interface with the metal electrodes could influence the inductor phase and promote stabilization of the radical cation segment in the P3HT polymer matrix after synthesis and during the assessment period. Figure 5 shows Raman spectra obtained at different times after synthesis for the Pt/PDPA/P3HT, ITO/PDPA/P3HT, and Au/PDPA/P3HT systems.

Figure 5a shows the Raman spectra obtained for the Pt/PDPA/P3HT system at the different assessment times. The spectrum obtained immediately after synthesis (Fig. 5a(a)) shows bands related to the radical cation (1204 cm^{-1} and 1325 cm^{-1}), a shadow associated with the dication segment (1585 cm^{-1}), and a band (1608 cm^{-1}) related to the PDPA aromatic ring. However, these bands had disappeared at 5 h after synthesis. The band at 1459 cm^{-1}, characteristic of C=C symmetric stretching of the P3HT thiophene ring, exhibited some variations in frequency and intensity depending on the time at which the spectra were recorded, and after 97 h had elapsed, this band was predominant over the others. This variation could be due to the intensification of the Raman signal for the segments present in P3HT, probably associated with semiquinone forms. The radical cation segment reached its maximum absorption at 677 nm in the UV–Vis spectrum.[24] This widened band is close to the Raman spectrum excitation wavelength (532 nm) and is thus intensified by the preresonance Raman effect when the species is predominant in the polymer matrix.

After deconvoluting the spectrum from 1420 cm^{-1} to 1490 cm^{-1} (Fig. 5a, inset), signals were observed at wavenumbers of 1435 cm^{-1}, 1446 cm^{-1}, and 1461 cm^{-1}. These are thought to relate respectively to thiophene ring and dication and radical cation segments of P3HT, even though they are displaced, as previously observed for the Pt/P3HT system (Fig. 3a). However, in the deconvoluted spectrum after 97 h (Fig. 5b, inset), there was a predominance of the band at 1460 cm^{-1} in the spectrum from 1400 cm^{-1} to 1510 cm^{-1}, proving that the radical cation
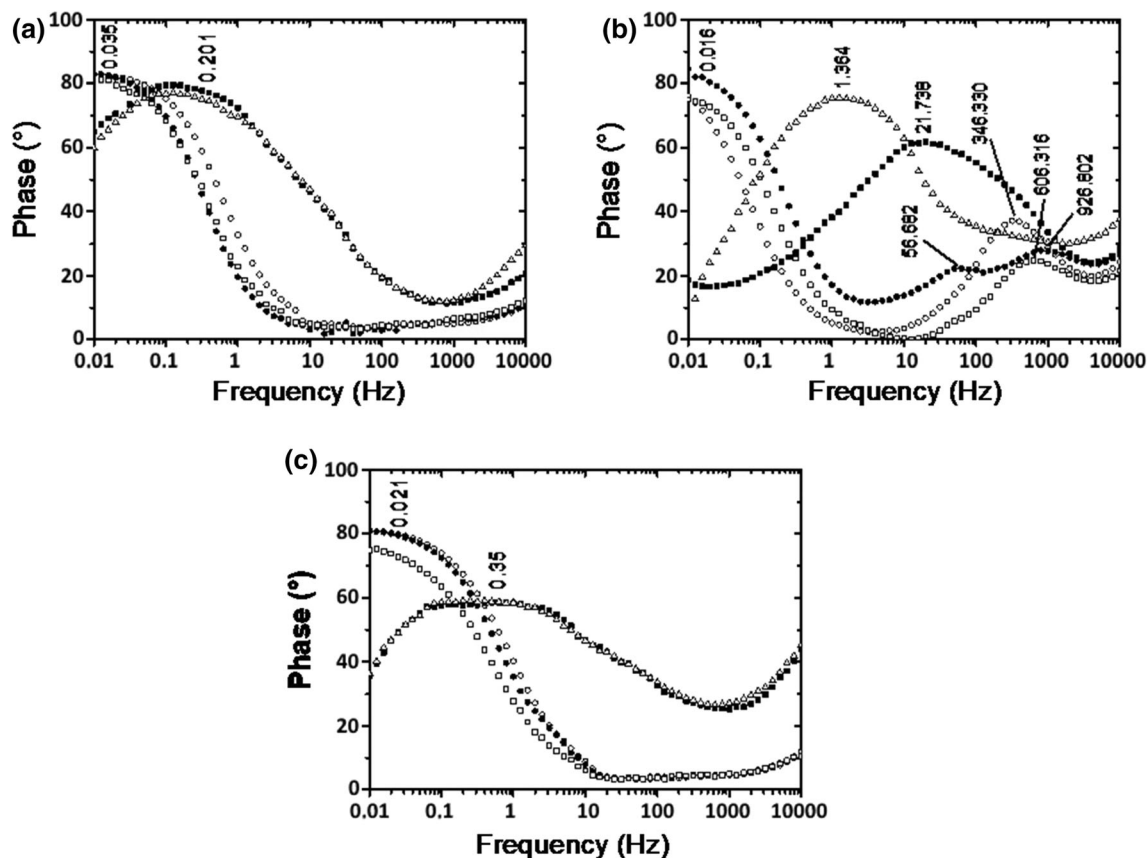
Fig. 4. Bode phase diagrams at open-circuit potential for (a) Pt/P3HT, (b) ITO/P3HT, and (c) Au/P3HT systems at 0 h (empty circle), 1 h (filled circle), 5 h (empty square), 48 h (filled square), and 97 h (empty triangle) after electrochemical synthesis.

segment stabilizes as time progresses. The displacement is probably due to the strong interactions between the charged layers of the PDPA and P3HT.

Figure 5b shows that the behavior of the spectra for the ITO/PDPA/P3HT system was similar to that seen in Fig. 5a at different time intervals. The deconvoluted band of P3HT in the as-prepared state (Fig. 5c, inset) exhibited signals related respectively to the aromatic, dication, and radical cation segments of the thiophene ring at wavenumbers of 1430 cm^{-1}, 1455 cm^{-1}, and 1475 cm^{-1}. After 97 h had elapsed, the band at 1456 cm^{-1} was still the most intense, and when it was deconvoluted (Fig. 5d, inset), only the bands at 1430 cm^{-1} and 1457 cm^{-1} remained, being related respectively to the P3HT aromatic and dication segments, proving that, as time elapsed, the dication and aromatic segments of this system stabilized.

Figure 5c shows the Raman spectra for the Au/PDPA/P3HT system, obtained at different times. These spectra exhibit a predominance of PDPA bands at 1202 cm^{-1}, 1319 cm^{-1}, 1530 cm^{-1}, and 1609 cm^{-1}, being related respectively to the radical cation and aromatic segments. The band at 1455 cm^{-1}, related to P3HT, appeared only after 97 h had elapsed. Deconvoluting this band revealed signals related to thiophene ring aromatic, dication, and radical cation segments at 1430 cm^{-1}, 1455 cm^{-1},

and 1475 cm^{-1}, indicating a higher contribution from the dication segment in the polymer matrix.

The latter results obtained by Raman spectroscopy were considered susceptible to error, mainly regarding the deconvolution of the P3HT band, induced by the instability exhibited on obtaining the spectrum, even at low laser intensity. This behavior can be understood in terms of the heat induced by increasing the laser power, as observed by Bento et al.[25] in a study on the photodegradation of P3OT. Using photoluminescence (PL) spectroscopy and the Raman technique, it was shown that the radical cation segments changed to quinone structures as a function of the laser exposure time.

Considering this limitation on the conditions for obtaining the Raman spectrum for this system, it was deemed necessary to use EIS to monitor the presence of radical cation segments in the polymer matrix. The results obtained using the Raman technique complemented those obtained by EIS.

Figure 6 shows the Bode phase diagrams, constructed based on the EIS data obtained for the Pt/PDPA/P3HT, ITO/PDPA/P3HT, and Au/PDPA/P3HT systems in 0.100 mol L^{-1} LiClO$_4$-ACN. The EIS measurements were taken at open-circuit potential (OCP) and constant temperature of 22°C after 0 h, 1 h, 5 h, 48 h, and 97 h had elapsed
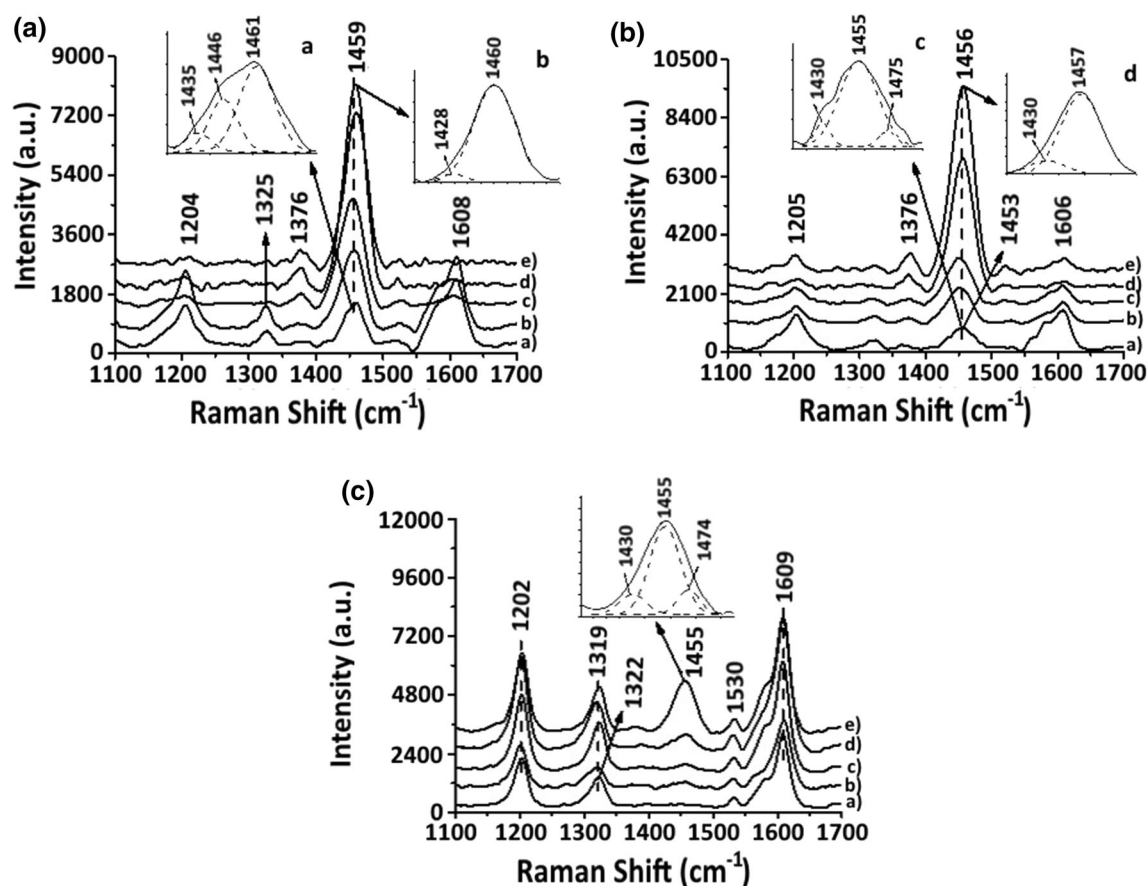
Fig. 5. Raman spectra with excitation at 532 nm for (a) Pt/PDPA/P3HT, (b) ITO/PDPA/P3HT, and (c) Au/PDPA/P3HT systems at (a) 0 h, (b) 1 h, (c) 5 h, (d) 48 h, and (e) 97 h after electrochemical synthesis.

following film synthesis on the Pt, ITO and Au electrodes.

Figure 6a shows a single phase at low frequency ($\sim$ 0.017 Hz), related to the polaron conduction charge-transfer process at all assessment times, confirming the stabilization of the radical cation segments at the interface between PDPA/P3HT and platinum. This behavior differs from that observed by Bento et al.,[13] who showed that, for systems containing P3MT and P3OT, there are two clearly defined phases, characteristic of the radical cation and dication.

These results can be used to corroborate the results obtained by the Raman technique, where there is a predominance of the band at 1460 cm^{-1} after 97 h. Stabilization of the radical cation segment as time elapses could indicate strong interactions between the charged layers of PDPA and P3HT, in contrast to the behavior observed for the radical cation segment at the Pt/P3HT interface.

Figure 6b shows the numerous phases as time elapsed, evidencing high instability of the interface with the ITO electrode, since the initial observations revealed a low-frequency ($\sim$ 0.012 Hz) phase related to the polaron conductance charge-transfer process, and after 1 h had elapsed there was a phase

at $\sim$ 3.873 Hz related to the bipolaron conduction charge-transfer process. However, after 5 h had elapsed, there were two phases, one at low frequency ($\sim$ 0.012 Hz) and the other at high frequency ($\sim$193.707 Hz), providing evidence of the formation of both radical cations and dications. After 48 h, the polymer engendered at this interface once again exhibited stabilization of only the dication segment at $\sim$ 6.419 Hz, and after 97 h the system exhibited only one widened phase at $\sim$ 0.943 Hz, indicating a mixture of radical cation and dication segments. Working on P3MT, de Lima et al.[14] obtained different results. They found that the radical cation segment was stable up to 20 h after synthesis, while after 24 h another high-frequency phase appeared, related to the dication segment, but with low intensity.

Figure 6c shows two low-frequency phases at $\sim$ 0.015 Hz and $\sim$ 0.033 Hz after 48 h, related to polaron charge-transfer processes, indicating that, up to this time, there is some stability of the radical cation, but after 97 h, a high-frequency phase appears at $\sim$ 6.392 Hz, indicating dication formation and confirming the results obtained by Raman spectroscopy (replacement of radical cation by dication segments in the matrix).

Electrical and Structural Characterization of Poly(3-hexylthiophene)–Polydiphenylamine
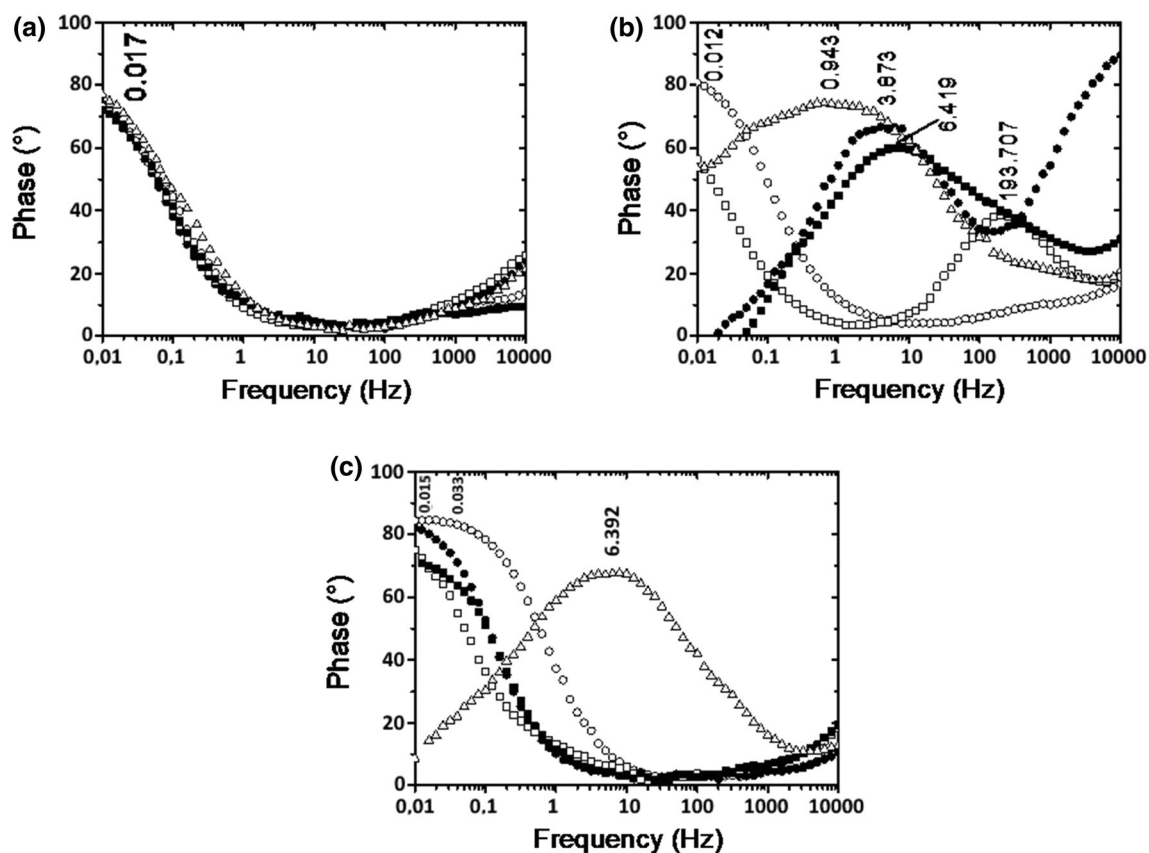Blends Synthesized on Various Conductive Substrates

Fig. 6. Bode phase diagrams at open-circuit potential for (a) Pt/PDPA/P3HT, (b) ITO/PDPA/P3HT, and (c) Au/PDPA/P3HT systems at 0 h (empty circle), 1 h (filled circle), 5 h (empty square), 48 h (filled square), and 97 h (empty triangle) after electrochemical synthesis.

CONCLUSIONS

EIS and Raman spectroscopy were applied to monitor the charge-transfer processes in these systems deposited on different conductive substrates. The system with the best radical cation segment stabilization was the Pt/PDPA/P3HT interphase, which remained effective for up to 97 h. The other systems (Au and ITO/PDPA/P3HT) were more favorable for the stabilization of dication segments.

With regard to the systems consisting of PDPA homopolymer alone, on Pt the system exhibited radical cation decay as time progressed, and a quantitative increase in the dication segment, indicating spontaneous disproportionation of radical cation segments. In contrast, at the ITO and Au interfaces, the system showed enhanced stabilization of the radical cation segment at all assessment times.

In the systems containing the P3HT homopolymer deposited on Pt and Au, the interfaces showed that the radical cation segment attempted to reach equilibrium with the dication segment as time progressed, and during the period up to 97 h, both segments were present in the matrices of these systems. However, the system consisting of the ITO electrode and P3HT homopolymer exhibited better equilibrium with the dication segment in the polymer matrix, showing some instability after 5 h, but a predominance of the high-frequency phase related to the dication segment.

Therefore, the interphase of P3HT with PDPA deposited on a Pt electrode exhibited a favorable charge inductor effect in the PDPA, mainly compared with the behavior of the Pt/P3HT system. These findings help elucidate how such systems could be used efficiently in the active layer of organic photovoltaic cells.

ACKNOWLEDGMENTS

CONFLICT OF INTEREST

The authors declare that they have no conflicts of interest.

REFERENCES

1. R. Faez, C. Reis, P.S. Freitas, O.K. Kosima, G. Ruggeri, and M.D. Paoli, R. Faez, C. Reis, P.S. Freitas, O.K. Kosima, G. Ruggeri, and M.D. Paoli, *Quim. Nova Esc.*, 2000, **11**, p 13.

2. H. de Santana, M.L.A. Temperini, and J.C. Rubim, H. de Santana, M.L.A. Temperini, and J.C. Rubim, *J. Electroanal. Chem.*, 1993, **356**, p 145.

3. A.G. Macdiarmid, A.G. Macdiarmid, *Synth. Met.*, 2001, **40**, p 2581.

4. F. Chen, P. Liu, and Q. Zhao, F. Chen, P. Liu, and Q. Zhao, *Electrochim. Acta*, 2012, **76**, p 62.

5. J. Hou, Z. Liu, and P. Zhang, J. Hou, Z. Liu, and P. Zhang, *J. Power Sources*, 2013, **224**, p 139.

6. P.J. Kulesza, K. Karnicka, K. Miecznikowski, M. Chojak, A. Kolary, P.J. Barczuk, G. Tsirlina, and W. Czerwinski, P.J. Kulesza, K. Karnicka, K. Miecznikowski, M. Chojak, A. Kolary, P.J. Barczuk, G. Tsirlina, and W. Czerwinski, *Electrochim. Acta*, 2005, **50**, p 5155.

7. Y.L. Lee, H.J. Tsai, and L.H. Chen, Y.L. Lee, H.J. Tsai, and L.H. Chen, *J. Mater. Chem.*, 2009, **19**, p 5778.

8. S.P. Palaniappan, and P. Manisankar, S.P. Palaniappan, and P. Manisankar, *Electrochim. Acta*, 2011, **56**, p 6123.

9. A. Bou, P. Torchio, S. Vedraine, D. Barakel, B. Lucas, J.-C. Bernède, P.-Y. Thoulon, and M. Ricci, A. Bou, P. Torchio, S. Vedraine, D. Barakel, B. Lucas, J.-C. Bernède, P.-Y. Thoulon, and M. Ricci, *Sol. Energy Mater. Sol. Cells.*, 2014, **125**, p 310.

10. L.M. Chen, Z.R. Hong, G. Li, and Y. Yang, L.M. Chen, Z.R. Hong, G. Li, and Y. Yang, *Adv. Mater.*, 2009, **21**, p 1434.

11. J. Mikroyannidi, A.N. Kabanakis, S.S. Sharma, and G.D. Sharma, J. Mikroyannidi, A.N. Kabanakis, S.S. Sharma, and G.D. Sharma, *Adv. Funct. Mater.*, 2011, **21**, p 746.

12. P. Vanlaeke, A. Swinnen, I. Haeldermans, G. Vanhoyland, T. Aernouts, D. Cheyns, C. Deibel, and J.P.J.S.J.V. D'haenHeremansPoortmanManca, P. Vanlaeke, A. Swinnen, I. Haeldermans, G. Vanhoyland, T. Aernouts, D. Cheyns, C. Deibel, and J.P.J.S.J.V. D'haenHeremansPoortmanManca, *J. Sol. Energy Mater. Sol. Cells.*, 2006, **90**, p 2150.

13. D.C. Bento, E.C.R. Maia, P.R.P. Rodrigues, G.J. Moore, G. Louarn, and H. de Santana, D.C. Bento, E.C.R. Maia, P.R.P. Rodrigues, G.J. Moore, G. Louarn, and H. de Santana, *J. Mater Sci: Mater Electron.*, 2013, **24**, p 4732.

14. J.H.C. de Lima, D.F. Valezi, A.D. Batista, D.C. Bento, and H. de Santana, J.H.C. de Lima, D.F. Valezi, A.D. Batista, D.C. Bento, and H. de Santana, *J. Mater Sci: Mater Electron.*, 2018, **29**, p 6511.

15. A.D. Batista, D.C. Bento, and H. De Santana, A.D. Batista, D.C. Bento, and H. De Santana, *J. Mater Sci: Mater Electron.*, 2017, **28**, p 1514.

16. G.M. do Nascimento, J.E.P. Silva, S.I.C. Torresi, and M.L.A. Temperini, G.M. do Nascimento, J.E.P. Silva, S.I.C. Torresi, and M.L.A. Temperini, *Macromolecules*, 2002, **35**, p 121.

17. D.C. Bento, E.C.R. Maia, T.N.M. Cervantes, R.V. Fernandes, E. Di Mauro, E. Laureto, M.A.T. da Silva, J.L. Duarte, I.F.L. Dias, and H. de Santana, D.C. Bento, E.C.R. Maia, T.N.M. Cervantes, R.V. Fernandes, E. Di Mauro, E. Laureto, M.A.T. da Silva, J.L. Duarte, I.F.L. Dias, and H. de Santana, *Synth. Met.*, 2012, **162**, p 2433.

18. D.C. Bento, G. Louarn, and H. de Santana, D.C. Bento, G. Louarn, and H. de Santana, *J. Mater Sci: Mater Electron.*, 2016, **27**, p 5371.

19. H. Koizumi, H. Dougauchi, and T. Ichikawa, H. Koizumi, H. Dougauchi, and T. Ichikawa, *J. Phys. Chem. B.*, 2005, **109**, p 15288.

20. S. Quillard, G. Louarn, J.P. Buisson, S. Lefrant, J. Masters, and A.G. MacDiarmid, S. Quillard, G. Louarn, J.P. Buisson, S. Lefrant, J. Masters, and A.G. MacDiarmid, *Synth. Met.*, 1992, **49–50**, p 525.

21. M.M. Kubota, B.L. Sacco, D.C. Bento, and H. de Santana, M.M. Kubota, B.L. Sacco, D.C. Bento, and H. de Santana, *Spec. Acta Part A: Mol. Biom. Spec.*, 2015, **151**, p 80.

22. G. Lillie, P. Payne, and P. Vagdama, G. Lillie, P. Payne, and P. Vagdama, *Sens. Actuators, B.*, 2001, **78**, p 249.

23. T.N.M. Cervantes, E.C.R. Maia, D.C. Bento, E. Laureto, D.A.M. Zaia, M.A.T. da Silva, G.J. Moore, and H. de Santana, T.N.M. Cervantes, E.C.R. Maia, D.C. Bento, E. Laureto, D.A.M. Zaia, M.A.T. da Silva, G.J. Moore, and H. de Santana, *J. Mater Sci: Mater Electron.*, 2012, **23**, p 1916.

24. D.C. Bento, T.N.M. Cervantes, E.C.R. Maia, C.A. Olivati, G. Louarn, and H. de Santana, D.C. Bento, T.N.M. Cervantes, E.C.R. Maia, C.A. Olivati, G. Louarn, and H. de Santana, *J. Mater Sci: Mater Electron.*, 2015, **26**, p 149.

25. D.C. Bento, E.C.R. Maia, R.V. Fernandes, E. Laureto, G. Louarn, and H. de Santana, D.C. Bento, E.C.R. Maia, R.V. Fernandes, E. Laureto, G. Louarn, and H. de Santana, *J. Mater. Sci: Mater. Electron.*, 2014, **25**, p 185.